HHS Public Access

Author manuscript

*Microcirculation*. Author manuscript; available in PMC 2018 July 01.

Published in final edited form as:

*Microcirculation*. 2017 July ; 24(5): . doi:10.1111/micc.12372.

# Cdc42 regulates branching in angiogenic sprouting in vitro

**Duc-Huy T. Nguyen**[1], **Lin Gao**[2], **Alec Wong**[3], and **Christopher S. Chen**[1,3,4,*]

[1]Department of Chemical and Biomolecular Engineering, University of Pennsylvania, Philadelphia, Pennsylvania 19104, USA

[2]Department of Bioengineering, University of Pennsylvania, Philadelphia, Pennsylvania 19104, USA

[3]Department of Biomedical Engineering, Boston University, Boston, Massachusetts 02215, USA

[4]Wyss Institute for Biologically Inspired Engineering, Harvard University, Boston, Massachusetts 02115, USA

## Abstract

**Objectives—**The morphogenetic events that occur during angiogenic sprouting involve several members of the Rho family of GTPases, including Cdc42. However, the precise roles of Cdc42 in angiogenic sprouting have been difficult to elucidate owing to the lack of models to study these events *in vitro*. Here, we aim to identify the roles of Cdc42 in branching morphogenesis in angiogenesis.

**Methods—**Using a 3D biomimetic model of angiogenesis *in vitro*, where endothelial cells were seeded inside a cylindrical channel within collagen gel and sprouted from the channel in response to a defined biochemical gradient of angiogenic factors, we inhibited Cdc42 activity with a small molecule inhibitor ML141 and examined the effects of Cdc42 on the morphogenetic processes of angiogenic sprouting.

**Results—**We find that partial inhibition of Cdc42 had minimal effects on directional migration of endothelial cells, but led to fewer branching events without affecting the length of these branches. We also observed that antagonizing Cdc42 reduced collective migration in favor of single cell migration. Additionally, Cdc42 also regulated the initiation of filopodial extensions in endothelial tip cells.

**Conclusions—**Our findings suggest that Cdc42 can affect multiple morphogenetic processes during angiogenic sprouting and ultimately impact the architecture of the vasculature.

### Keywords

Cdc42; branching; angiogenesis; biomimetic model; filopodia

*Corresponding author: chencs@bu.edu.

**Authors' contribution:**

DHTN, LG, and AW designed and performed the experiments. DHTN and AW analyzed the data. DHTN, CSC wrote the manuscript. CSC conceptually designed and supervised the project.

**Conflict of interest:**

The authors declare no conflicts of interest.

## Introduction

Angiogenesis is a process where new blood vessels form from existing vasculature. Endothelial cells from capillaries respond to angiogenic cues by extending filopodial protrusions, digesting the vascular basement membrane, and invading into the interstitial matrix as tip cells with following stalk cells (1). These multicellular sprouts eventually develop into mature perfusable blood vessels with hierarchical, branched architectures (2). To establish these ordered vessel networks, sprouts first extensively branch, reconnect, and undergo changes such as pruning to remodel the structures. All these processes require dynamic changes in cytoskeleton of endothelial cells.

Rho GTPase proteins are known to regulate actin cytoskeletal dynamics in cell migration during organ development and tissue morphogenesis (3). Among Rho GTPase proteins, Cdc42 has a conserved role in regulating actin cytoskeleton dynamics, filopodial extensions, cell polarity, and migration (3). In neuronal cells, deletion of Cdc42 reduces branching of growth cones (4, 5). *In vivo* deletion of Cdc42 whether via germ-line or endothelial-cell-specific knockout, results in major defects in vascular formation in both fetal and adult vasculatures. For example, the vascular network lacks branched structures in the trunk and the heart of mice lacking Cdc42 (6). Despite such obvious phenotype, it is, however, difficult to decipher whether these effects are a result of defects in vasculogenesis or angiogenesis. In culture models of vasculogenesis, a process where endothelial cells spontaneously assemble into networks, Cdc42 appears to be important in lumen formation (7). In contrast, its role in angiogenesis remains, however, poorly understood, due to the lack of equivalent culture models of angiogenic sprouting.

Recently, we have developed an *in vitro* model wherein endothelial cells lining a perfusable lumen can be induced with angiogenic factors to sprout and invade into the surrounding extracellular matrix (8). In this model, many of the morphogenic features of sprouting angiogenesis are recapitulated, including tip cells, stalk cells, and multicellular branched networks. Here, using this system, we sought to investigate the effects of Cdc42 on the morphogenic processes of angiogenesis. Unlike other studies of tubulogenesis and Matrigel™ assays, where endothelial cell network formation occurred in a uniform distribution of biochemical stimuli, our system employed a biochemical gradient not only to stimulate the formation of multicellular sprout structures, but also to unveil the effects of Cdc42 in the context of chemotactic migration in angiogenic sprouting. We observed that Cdc42 mediates several aspects of the morphogenetic processes of angiogenesis.

## Materials and Methods

### Device fabrication

As previously reported, devices were fabricated from two layers of poly(dimethylsiloxane) (PDMS; Sylgard 184; Dow-Corning), which were cast from silicon wafer masters (8). The PDMS layers were treated with a plasma etcher (Quorum Technologies), bonded together and adhered to a 25mm square glass coverslip. After treatment with 0.1mg/ml poly-L-lysine (Sigma) for 1hr, they were treated with 1% glutaraldehyde for 1hr and washed several times with water. Rat tail collagen type I (2.5mg/ml, Corning) solution was pipetted into the

devices with two 400μm diameter acupuncture needles. Upon gelation, the needles were extracted leaving two hollow cylindrical channels within the collagen matrix.

### Cell culture

Human umbilical vein endothelial cells (HUVECs) (Lonza) were cultured in EGM-2 (Lonza) up to passage 9. HUVECs were seeded into the channel at $3\times10^6$ cells/mL as previously described (8). After seeding was complete, devices were immediately placed on a platform rocker (BenchRocker, BR2000).

### Angiogenic sprouting assay

A combination of angiogenic factors including vascular endothelial growth factor (VEGF, 75ng/ml, R&D), monocyte chemotactic protein-1 (MCP-1, 75ng/ml, R&D), sphingosine-1-phosphate (S1P, 500nM, Cayman Chemical) and Phorbol Myristate Acetate (PMA, 10ng/ml, Sigma) were administered the day after cell seeding. The cocktail of angiogenic factors was refreshed daily as previously described (8).

### Inhibition of Cdc42 experiment

The day after cell seeding, the angiogenic cocktail of VEGF, MCP-1, S1P, and PMA was administered into the angiogenic source channel to trigger angiogenic sprouting. Simultaneously, the Cdc42 inhibitor (ML141, 15μM, Millipore) was administered in both the biomimetic blood vessel and in the angiogenic source channel at the onset of sprouting. Devices were either treated with DMSO as control or ML141 over a course of 4 days before they were fixed and stained for confocal imaging. Devices were always placed on a tilting rocker to provide shear forces in the channels over the entire course of experiments. For filopodia experiment, 22.5μM ML141 was added for 4 hours before they were fixed for quantification (N=4 individual experiments).

### Immunofluorescence and confocal image acquisition

After fixation, devices were permeated with 0.1% Triton-X (Sigma) for 30min and proceeded to incubation with Phalloidin Alexa 488 (1:200, Invitrogen) overnight in the cold room. The devices were washed several times with 1xPBS until fluorescent background was negligible before image acquisition. Confocal images were acquired with 40× water immersion objective, Axiovert 200M inverted microscope (Zeiss), a CSU-X1 spinning disk confocal scan head (Yokogawa Electric Corporation), and iXon3 897 EMCCD camera (Andor Technology). Images were acquired in a tiling mode and stitched using ImageJ (9).

### Quantification of the distance of invading cells

To quantify the distance of invading cells, we used a custom Matlab code to measure the distance of the invading cells from the parent vessel. The invading cells included both migrating sprout tip cells and migrating single cells from our phase contrast images.

### Quantification of sprout length, sprout density, sprout angle, and the number of invading cells

To quantify sprout length, we utilized high magnification microscopy (40× objective) to capture 3D sprouts in their entirety and performed Z-projection of confocal image stacks. A custom MATLAB code was written to measure the individual distances from the leading protrusions of only sprout tip cells to the wall of the parent vessel from the Z-projection images of sprouts. To quantify sprout density, another Matlab code was written to count the number of sprouts over a unit area of 300μm$^2$ in Z-projection of confocal image stack. Sprout angle was determined as the angle from which a sprout deviates from the vertical direction of the gradient between the two channels. ImageJ was used to count the number of cell nuclei from projections of Z-resolved confocal stacks. (N = 4 individual experiments).

### Quantification of branches and intersegmental branches

Adopting the custom MATLAB code from quantification of sprouts, we quantified the number of branches and intersegmental branches and their respective lengths. A branch length was defined as the distance from the tip of the branch to the end of the branch on the parent vessel, whereas intersegmental branch length was defined as the distance connecting the two ends of the intersegmental branch on two separate sprouts.

### Filopodia quantification

A custom MATLAB code was used to determine the distance from the tips of filopodia to where they originate on the cell body from projections of Z-resolved confocal stacks. The number and length of filopodia were averaged over the number of tip cells in each sample. Filopodia angle was measured as the angles in which a filopodium deviates from the vertically perpendicular line between the 2 channels (N=4 individual experiments).

### Statistical analysis

Sample populations were compared using unpaired, two-tailed Student’s t-test or two-sided Wilcoxon rank sum test. Data points on the graphs represent average values and error bars depict SEM. * ($p<0.05$), ** ($p<0.01$) and *** ($p<0.001$) indicate statistical significance.

## Results

### Inhibition of Cdc42 reduced 3D invasion speed of sprouts

To elucidate the role of Cdc42 in angiogenesis, we employed a biomimetic angiogenic model which we previously developed (Figure 1A). Briefly, the system consists of two hollow cylindrical channels embedded within a 3D collagen matrix, which are formed by polymerizing a solution of rat tail collagen I around acupuncture needles that are later removed. In one of the channels, endothelial cells were seeded to form an endothelium. In the second channel, a cocktail of angiogenic factors was administered to establish an angiogenic gradient to trigger sprouting into the 3D collagen matrix (8). Genetic manipulation of Cdc42 with a dominant negative Cdc42N17 appeared to inhibit formation of a monolayer of endothelial cells with intact junctional contacts in our channel and inhibit cell migration. Therefore, to inhibit Cdc42 activity, cultures were treated with a selective

pharmaceutical inhibitor of Cdc42 ML141 after monolayer formation (10, 11). In the pilot experiments, we observed that complete inhibition of Cdc42 using high concentrations of ML141 led to rapid cell death (Supplementary Figure S1). Therefore, to enable our studies, we targeted a 50% decrease in the activity of Cdc42 (Figure 1B). To maximize the effect of Cdc42 inhibition on sprouting morphogenesis, we administered the inhibitor at the onset of sprouting and monitored the migration of endothelial cells using phase contrast imaging over a course of 4 days. We quantified the distance traveled by invading cells into the interstitial collagen matrix and showed that partial inhibition of Cdc42 activity appeared to significantly slow down the invasion speed and migration of endothelial cells into the interstitial matrix (Figure 1C), suggesting that Cdc42 regulates migration speed of angiogenic sprouting.

## Inhibiting Cdc42 diminished sprout density and sprout length

To further characterize the effects of Cdc42 inhibition on sprouting, we queried whether there were observable changes to the structure of the multicellular sprouts themselves, which could not be examined under phase contrast microscopy imaging. Thus, after sprouting for 4 days, cultures with and without ML141 were fixed, stained, and imaged using confocal microscopy. The high resolution of the confocal images of 3D sprouts enabled careful inspection of the multicellular sprout structures and integrity. Although partial inhibition of Cdc42 slightly decreased the number of sprouts per unit area of parent vessel (Figure 2A), its effect was more pronounced on the average sprout length. We observed that the average sprout length was reduced by nearly half when Cdc42 was partially inhibited (Figure 2B), suggesting a role of Cdc42 in the extension of multicellular sprouts.

Given that Cdc42 regulates cell polarity, and persistence of migration on 2D substrates (10, 12), we hypothesize that inhibition of Cdc42 may reduce directional migration in a 3D collagen matrix. As a metric for directional migration, we measured the sprout angle as the deviation angle of the sprout from vertical axis between the two channels. In our model, addition of ML141 did not alter the sprout angle suggesting that directional migration was maintained (Figure 2C). Interestingly, the number of migrating cells significantly decreased when Cdc42 activity was antagonized (Figure 2D). Examining the migrating cells in the interstitial matrix, we observed a fraction of the migrating cells were single cells, and this fraction was significantly elevated when Cdc42 activity was diminished (Figure 2E, F). Moreover, we also observed that junctional contacts of endothelial cells were also compromised when they were exposed to the Cdc42 inhibitor (Supplementary Figure S2). Interestingly, Cdc42 has been implicated in regulating lumen formation in endothelial cell tubulogenesis, but our data demonstrated that the percentage of lumenized sprouts remained unaffected when Cdc42 activity was partially blocked (Supplementary Figure S3). Taken together, these data unveiled that partial inhibition of Cdc42 activity reduced the extent of cellular invasion and impaired collective cell migration during angiogenic sprouting, possibly due to compromising junctional contacts in endothelial cells.

## Cdc42 regulates branching morphogenesis of angiogenic sprouting

During angiogenesis, blood vessel branching is an important morphogenetic process to grow complex vascular networks (2, 13). As previously reported, branching was evidenced in our

3D biomimetic angiogenic model (8). We observed two distinct populations of branches in our model. One set of multicellular branches exhibit multicellular structures that emanate from a multicellular sprout, whereas another set of multicellular branches appear to connect two neighboring sprout structures, which we referred to as intersegmental branches (Figure 3A). A careful examination of the multicellular sprout structures in our model using confocal microscopy images disclosed that a majority of sprouts exhibited one branch point, suggesting that most multicellular sprouts exhibit either a single branch or a single intersegmental branch (Figure 3B). Moreover, inhibition of Cdc42 activity significantly reduced the number of branches by nearly half (Figure 3B). To further investigate how Cdc42 affects the branches and intersegmental branches, we quantified the quantity and the length of the multicellular branched structures. Antagonizing Cdc42 significantly reduced the formation of branches and intersegmental branches by suppressing the fraction of sprouts with multicellular branched structures (Figure 3C, D). Surprisingly, the length of both branches and intersegmental branches remained unaltered upon partial inhibition of Cdc42 activity (Figure 3E, F). Together this suggests that Cdc42 enables endothelial cells to initiate new branches, but does not participate in regulating extension of the branches and intersegmental branches.

### Effects of Cdc42 inhibition on filopodia formation

One possibility for how Cdc42 promotes branching is through its reported effects on filopodial formation, mostly described for cells cultured in 2D settings (14–16). To investigate whether Cdc42 is involved in filopodial formation in 3D, we treated well developed multicellular sprout structures with defined tip cells (Figure 4A,i) with an acute dose of the inhibitor ML141 at day 3. Exposure to Cdc42 inhibitor ML141 on these invading angiogenic sprouts revealed acute changes in filopodia appearance (Figure 4A,i and ii). Utilizing high resolution confocal microscopy images of the tip cells, we detected that ML141 did not alter the orientation of filopodia-like extensions towards the angiogenic stimuli (Figure 5B), consistent with our observations that sprouts remained oriented towards the angiogenic gradient regardless of ML141 exposure. Surprisingly, antagonizing Cdc42 doubled the number of filopodia-like extensions in tip cells (Figure 4C). Close inspection at the distribution of filopodia-like extensions per tip cells when Cdc42 activity was perturbed, we observed a sharp decline in the fraction of cells with less than 35 filopodia-like extensions, whereas a fraction of cells with more than 60 filopodia-like extensions upsurged (Figure 4D). These changes ultimately led to a surge in the number of filopodia-like extensions. Furthermore, perturbation of Cdc42 activity also significantly reduced the length of these filopodia-like extensions (Figure 4E) due to an upsurge in filopodia-like extensions of ~5 μm long (Figure 4F).

## Discussion

While Cdc42 has been identified as an important regulator of many cellular processes such as control of cell division, establishment of cellular polarity, and formation of filopodia in 2D cell culture (12, 17), its role in endothelial cells in 3D settings has only been explored in detail at the initiation and formation of lumen during tubulogenesis (7, 18). Using biomimetic blood vessels where endothelial cells were triggered to sprout by a defined

biochemical gradient, our results suggest that inhibition of Cdc42 affects different morphogenetic processes of endothelial cells during angiogenic sprouting.

Collective migration is a prevalent mode of migrating cells during mammalian morphogenesis (19). During collective migration, cohesive cells are held together through intercellular junctions (20). Cdc42 has been reported not only to affect cell migration, but also to establish junctional complexes within collective migrating cells (21, 22). For example, Cdc42 interacts with downstream protein complexes to regulate the formation of junctional proteins and maintain collective migration of hypodermal epithelial cells in Caenorhabditis elegans (23). Additionally, Cdc42 is activated by junctional proteins, P-cadherins, to mediate collective migration in mesenchymal myoblasts (24). In angiogenic sprouting, endothelial cells migrate collectively to drive the formation of the new blood vessels. In our model, partial inhibition of Cdc42 activity elevated the number of migrating single cells suggesting that Cdc42 activity was crucial in regulating and maintaining cell-cell contacts in multicellular sprouts in angiogenesis. Despite the crucial role of Cdc42 to mediate various cytoskeletal events during collective migration in angiogenesis, how Cdc42 interacts with downstream effectors to support cohesiveness of multicellular structures in angiogenesis remains largely unknown. Interestingly, a recent attempt to induce deletion of Cdc42 in embryonic endothelial cells reveals a pivotal function of Cdc42 to drive blood vessel formation and suggests that Cdc42 engages actin fibers to VE-cadherent junctions to establish the maturation of endothelial cell junctions (25). This leads us to postulate that during angiogenic sprouting, Cdc42 may also signal through VE-cadherent and actin fibers to stabilize the junctional complexes and maintain endothelial cell collective migration.

During lung development, Cdc42 directly regulates polarity and its activity is heightened at the active budding sides (26). Consequently, disruption of Cdc42 by genetic knockout causes abnormal Cdc42 activity on the epithelial cell layer and ultimately reduces epithelial cell budding during lung morphogenesis (26). Similarly, in endothelial cell sprouting from an endothelium, quiescent endothelial cells first need to reverse polarity to become tip cells (27). As a result, a disruption of polarity signaling may potentiate abnormal morphogenesis. Our result demonstrated that partial inhibition of Cdc42 activity caused a reduction in sprout density, which may suggest a role of Cdc42 to contribute to the initiation of tip cells from the endothelium. Similarly, the number of branches, where stalk cells have to emerge from sprouts to become tip cells, is also reduced. These results indicate that Cdc42 may act through cellular polarity to positively regulate the initiation of tip cell formation within an endothelium and within the stalk cells in the trunk of endothelial sprouts. As a result, disruption of Cdc42 signaling caused a reduction in the formation of sprouts and branches in angiogenic sprouting in our 3D biomimetic model.

One of the regulatory activities of Cdc42 is to mediate the formation of filopodia. In fibroblasts and neurons, inhibition of Cdc42 prevented formation of filopodia. However, in our 3D model, we observed that acute inhibition of Cdc42 upsurged the number of shorter filopodia-like extensions in endothelial tip cells. This observation suggested that Cdc42 activity at the leading edge of endothelial tip cells negatively regulated the initiation of filopodia formation. Interestingly, these short filopodial extensions were still directed towards the direction of the chemotactic gradient. This suggested that although Cdc42 has a

critical role in regulating the initiation of filopodia formation, direction of filopodial extensions in endothelial tip cells is regulated through a different mechanism in chemotactic migration. For example, during neutrophil migration, polarization signal was induced through recruitment and activation of PIP2/PIP3 to the front edge of neutrophils. This asymmetric accumulation of active PIP2/PIP3 signal establishes a stable polarity and strengthen the pseudopods to extend towards the chemoattractant (28, 29).

## Perspective

In conclusion, using an organotypic model of angiogenesis in which sprouting emanates from an endothelium under a defined biochemical gradient, we characterized the effects of Cdc42 on angiogenic sprouting using a pharmaceutical inhibitor of Cdc42 ML141. In our 3D angiogenic model, Cdc42 appeared to regulate branching morphogenesis, collective migration of endothelial cells, and negatively regulate the initiation of filopodia formation in tip cells, acknowledging the limitation that genetic modification of Cdc42 activity could not be used to confirm these findings. Additionally, since Cdc42 is essential for cell survival, how the morphogenesis of vessel sprouting is affected when Cdc42 activity is completely abolished remains to be explored, and likely would require alternative methods to manipulate Cdc42 activity in spatial and temporal manners. A concrete understanding of vessel branching and how it is regulated by Cdc42 will provide valuable insight into designing and engineering vascular networks to support functional tissue implants.

## Supplementary Material

Refer to Web version on PubMed Central for supplementary material.

## Acknowledgments

We thank Eyckmans, J. for helpful discussions. This work was supported in part by grants from the National Institutes of Health (EB00262).

## References

1. Gerhardt H, et al. VEGF guides angiogenic sprouting utilizing endothelial tip cell filopodia. J Cell Biol. 2003; 161(6):1163–1177. [PubMed: 12810700]
2. De Smet F, Segura I, De Bock K, Hohensinner PJ, Carmeliet P. Mechanisms of vessel branching: filopodia on endothelial tip cells lead the way. Arterioscler Thromb Vasc Biol. 2009; 29(5):639–649. [PubMed: 19265031]
3. Heasman SJ, Ridley AJ. Mammalian Rho GTPases: new insights into their functions from in vivo studies. Nat Rev Mol Cell Biol. 2008; 9(9):690–701. [PubMed: 18719708]
4. Govek EE, Newey SE, Van Aelst L. The role of the Rho GTPases in neuronal development. Genes Dev. 2005; 19(1):1–49. [PubMed: 15630019]
5. Chen TJ, Gehler S, Shaw AE, Bamburg JR, Letourneau PC. Cdc42 participates in the regulation of ADF/cofilin and retinal growth cone filopodia by brain derived neurotrophic factor. J Neurobiol. 2006; 66(2):103–114. [PubMed: 16215999]
6. Jin Y, et al. Deletion of Cdc42 enhances ADAM17-mediated vascular endothelial growth factor receptor 2 shedding and impairs vascular endothelial cell survival and vasculogenesis. Mol Cell Biol. 2013; 33(21):4181–4197. [PubMed: 23979594]

7. Bayless KJ, Davis GE. The Cdc42 and Rac1 GTPases are required for capillary lumen formation in three-dimensional extracellular matrices. J Cell Sci. 2002; 115(Pt 6):1123–1136. [PubMed: 11884513]
8. Nguyen DH, et al. Biomimetic model to reconstitute angiogenic sprouting morphogenesis in vitro. Proc Natl Acad Sci U S A. 2013; 110(17):6712–6717. [PubMed: 23569284]
9. Rasband, WS. ImageJ. National Institute of Health; Bethesda, Maryland, USA: 1997–2012.
10. Yamao M, et al. Distinct predictive performance of Rac1 and Cdc42 in cell migration. Sci Rep. 2015; 5:17527. [PubMed: 26634649]
11. Surviladze Z, et al. A Potent and Selective Inhibitor of Cdc42 GTPase. 2010
12. Etienne-Manneville S. Cdc42--the centre of polarity. J Cell Sci. 2004; 117(Pt 8):1291–1300. [PubMed: 15020669]
13. Carmeliet P, De Smet F, Loges S, Mazzone M. Branching morphogenesis and antiangiogenesis candidates: tip cells lead the way. Nat Rev Clin Oncol. 2009; 6(6):315–326. [PubMed: 19483738]
14. Chen F, et al. Cdc42 is required for PIP(2)-induced actin polymerization and early development but not for cell viability. Curr Biol. 2000; 10(13):758–765. [PubMed: 10898977]
15. Garvalov BK, et al. Cdc42 regulates cofilin during the establishment of neuronal polarity. J Neurosci. 2007; 27(48):13117–13129. [PubMed: 18045906]
16. Yang L, Wang L, Zheng Y. Gene targeting of Cdc42 and Cdc42GAP affirms the critical involvement of Cdc42 in filopodia induction, directed migration, and proliferation in primary mouse embryonic fibroblasts. Mol Biol Cell. 2006; 17(11):4675–4685. [PubMed: 16914516]
17. Johnson DI. Cdc42: An essential Rho-type GTPase controlling eukaryotic cell polarity. Microbiol Mol Biol Rev. 1999; 63(1):54–105. [PubMed: 10066831]
18. Koh W, Mahan RD, Davis GE. Cdc42- and Rac1-mediated endothelial lumen formation requires Pak2, Pak4 and Par3, and PKC-dependent signaling. J Cell Sci. 2008; 121(Pt 7):989–1001. [PubMed: 18319301]
19. Ilina O, Friedl P. Mechanisms of collective cell migration at a glance. J Cell Sci. 2009; 122(Pt 18): 3203–3208. [PubMed: 19726629]
20. Friedl P, Gilmour D. Collective cell migration in morphogenesis, regeneration and cancer. Nat Rev Mol Cell Biol. 2009; 10(7):445–457. [PubMed: 19546857]
21. Petronczki M, Knoblich JA. DmPAR-6 directs epithelial polarity and asymmetric cell division of neuroblasts in Drosophila. Nat Cell Biol. 2001; 3(1):43–49. [PubMed: 11146625]
22. Yamanaka T, et al. PAR-6 regulates aPKC activity in a novel way and mediates cell-cell contact-induced formation of the epithelial junctional complex. Genes Cells. 2001; 6(8):721–731. [PubMed: 11532031]
23. Ouellette MH, Martin E, Lacoste-Caron G, Hamiche K, Jenna S. Spatial control of active CDC-42 during collective migration of hypodermal cells in Caenorhabditis elegans. J Mol Cell Biol. 2016; 8(4):313–327. [PubMed: 26578656]
24. Plutoni C, et al. P-cadherin promotes collective cell migration via a Cdc42-mediated increase in mechanical forces. J Cell Biol. 2016; 212(2):199–217. [PubMed: 26783302]
25. Barry DM, et al. Cdc42 is required for cytoskeletal support of endothelial cell adhesion during blood vessel formation in mice. Development. 2015; 142(17):3058–3070. [PubMed: 26253403]
26. Wan H, et al. CDC42 is required for structural patterning of the lung during development. Dev Biol. 2013; 374(1):46–57. [PubMed: 23219958]
27. Lee CY, Bautch VL. Ups and downs of guided vessel sprouting: the role of polarity. Physiology (Bethesda). 2011; 26(5):326–333. [PubMed: 22013191]
28. Sasaki T, et al. Function of PI3Kgamma in thymocyte development, T cell activation, and neutrophil migration. Science. 2000; 287(5455):1040–1046. [PubMed: 10669416]
29. Van Keymeulen A, et al. To stabilize neutrophil polarity, PIP3 and Cdc42 augment RhoA activity at the back as well as signals at the front. J Cell Biol. 2006; 174(3):437–445. [PubMed: 16864657]

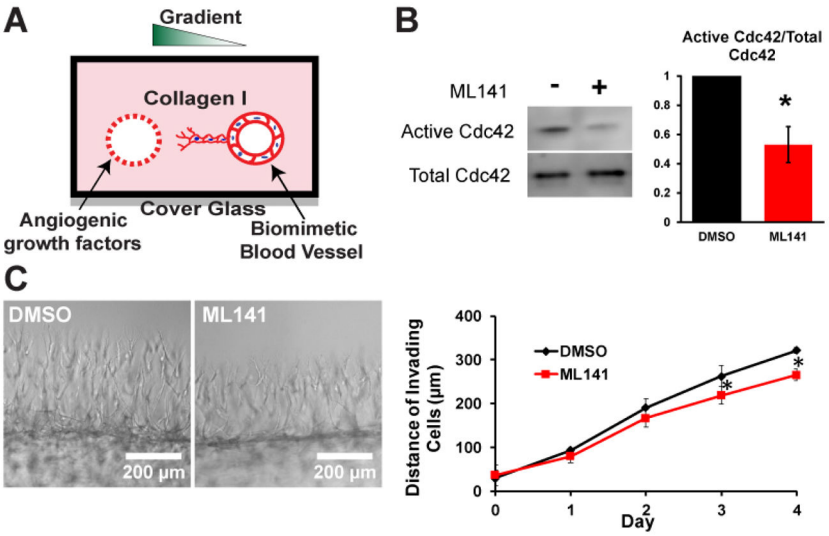


**Figure 1.**

Inhibition of Cdc42 in 3D biomimetic angiogenic model. (A) Schematic of our 3D biomimetic model of angiogenesis. A device is consisted of 2 channels fully embedded inside 2.5mg/ml collagen gel. (B) Cdc42 activity was reduced in half in the presence of 15 μM Cdc42 inhibitor ML141. (C) Representative phase images of sprouts guided by a gradient of angiogenic cocktail including MCP-1, VEGF, PMA, and S1P at Day 4 for control DMSO and Cdc42-inhibited devices. Average invading distance of invading cells into matrix was reduced in the presence of ML141 (N=4 individual experiments); * ($p<0.05$) indicates statistical significance.

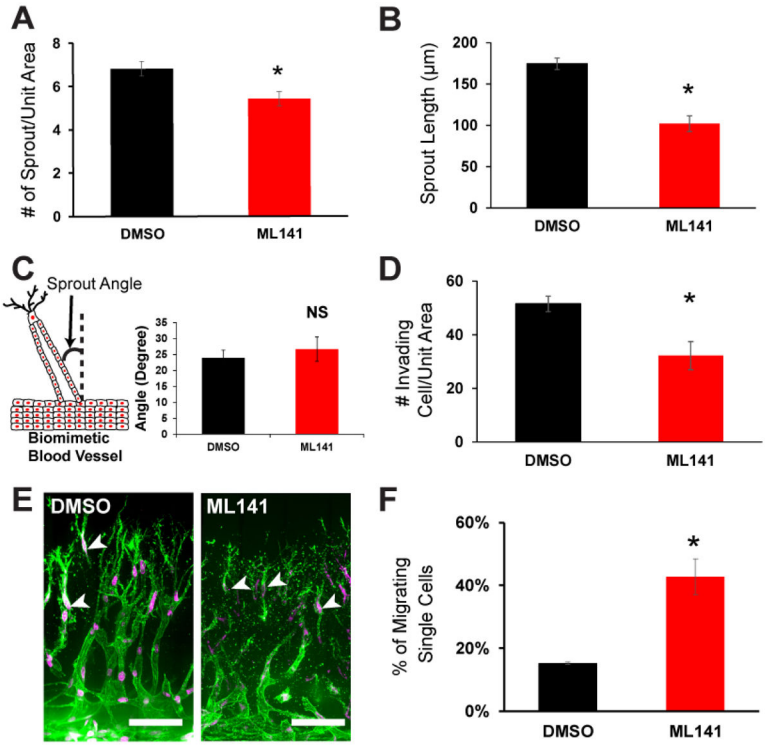


**Figure 2.**

The effects of Cdc42 on sprout length and density during angiogenesis sprouting. (A) Quantification of sprout density between control DMSO and Cdc42 inhibition conditions. ML141 was initiated at onset of sprouting over a course of 4 days (n=4 individual experiments). The presence of Cdc42 inhibitor slightly decreased the sprout density. (B) Sprout length was quantified at day 4 using images acquired from confocal microcopy. Sprout length was halved when Cdc42 activity was partially inhibited (n=4 individual experiments). (C) Quantification of average sprout angle between DMSO and ML141 devices (n=4 individual experiments) revealed unaltered directional migration of the multicellular sprout structures. (D) Quantification of the number of invading cells demonstrated inhibition of Cdc42 reduced migrating cells into the interstitial matrix (n=4 individual experiments). (E) Representative 3D projections of Z-stack confocal images of sprouts in DMSO and ML141 conditions at day 4. White arrowheads indicate single migrating cells. Scale bar is 100 μm. (F) Quantification of single cell migration among migrating cells in the interstitial matrix revealed a significant increase in the fraction of single migrating cells (n=4 individual experiments). Unit area is 300 $\mu m^2$. * indicates statistical significance ($P<0.05$); ns indicates no statistical significance.

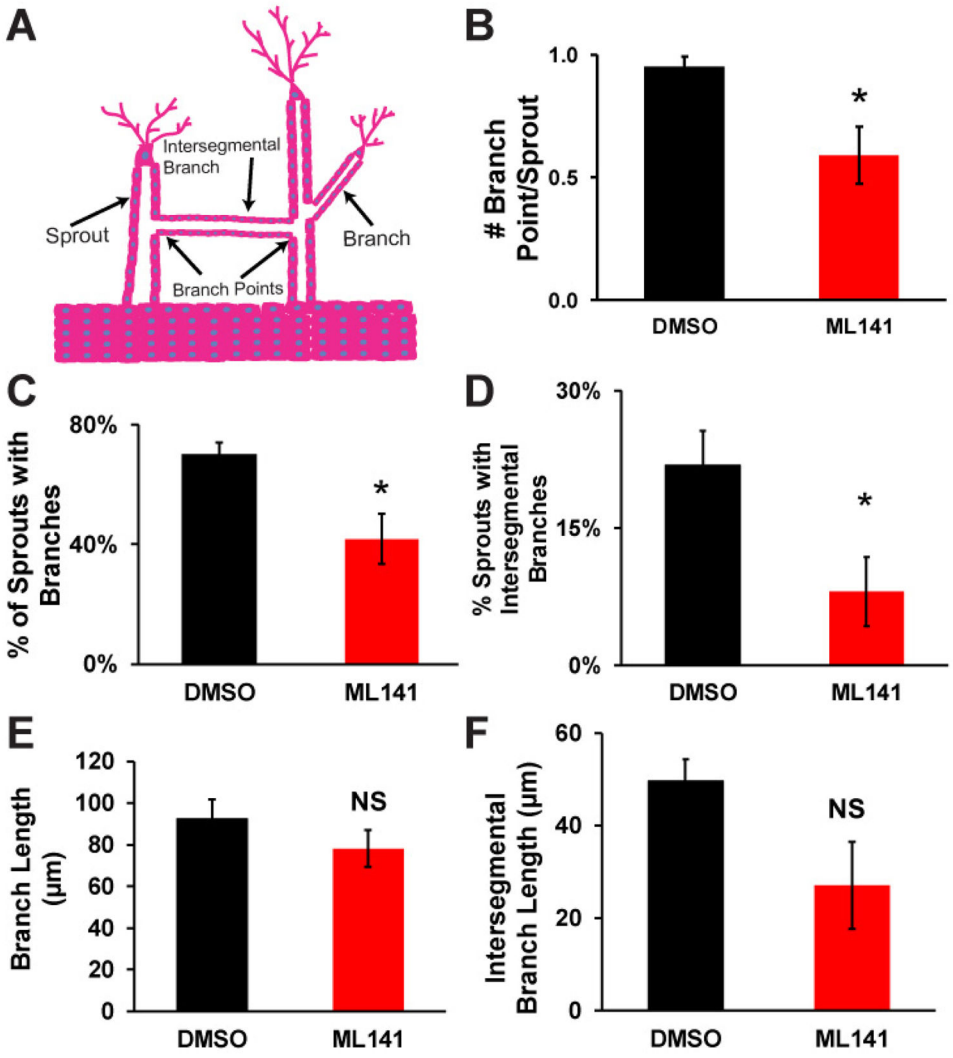


**Figure 3.**

The effects of antagonizing Cdc42 on branching morphogenesis of angiogenic sprouting. (A) A schematic of two different branching structures (branch and intersegmental branch) observed in angiogenic sprouting in our model guided by a gradient of angiogenic cocktail. (B) Number of branch points is quantified for DMSO vs ML141 conditions. (C) The fraction of sprouts with branches was reduced in the presence of ML141. (D) The fraction of sprouts with intersegmental branches was also reduced when Cdc42 activity was perturbed with ML141. (E) Average length of branch was unaffected by the inhibition of Cdc42. (F) Average length of intersegmental branches was also unaffected by the inhibition of Cdc42. N=4 individual experiments; * ($p<0.05$) indicates statistical significance; ns indicates no statistical significance.

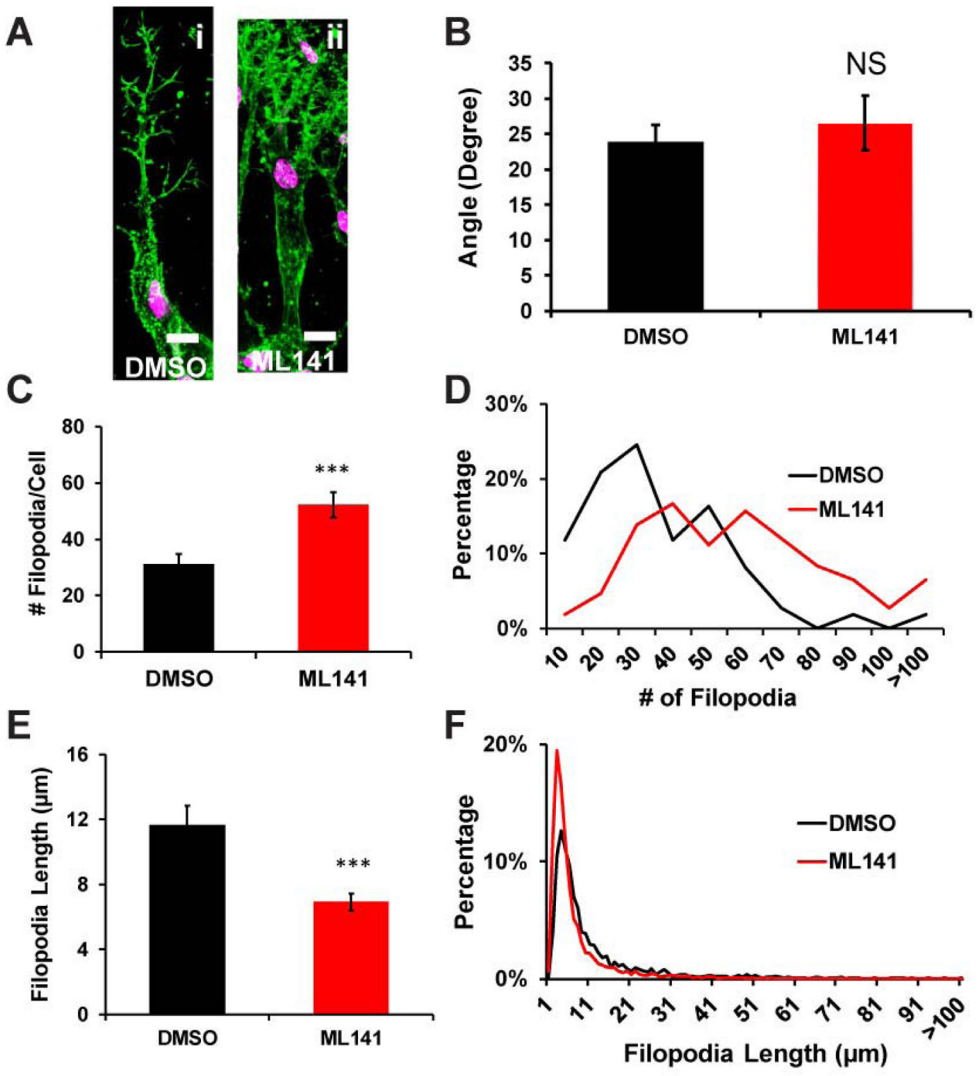


**Figure 4.**

Filopodia formation of endothelial cell sprouting upon Cdc42 inhibition. (A) Representative confocal images of phalloidin-stained sprout tip cells showing filopodia-like extensions in DMSO and ML141 conditions. Sprouting was initiated for 3 days. Then 22.5μM ML141 was added for 4hrs before fixation. (B) Average angle of filopodia of sprout tip cells remained unchanged upon inhibition of Cdc42 (n=4 individual experiments). (C) The number of filopodial extensions per sprout tip cells in DMSO and ML141 conditions (n=4 individual experiments) displayed a surge in filopodia-like extension in ML141 treatment. (D) Histogram showing distribution of the filopodia-like extension numbers per sprout tip cells for DMSO and ML141 conditions (n=4 individual experiments). (E) Average length of filopodia-like extensions is quantified for DMSO and ML141 conditions (n=4 individual experiments). (F) Histogram showing distribution of the length of the filopodia-like extensions for DMSO and ML141 conditions. * ($p<0.05$) and *** ($p< 0.001$) indicate statistical significance.